ISSN(Online): 2319-8753
ISSN (Print): 2347-6710

International Journal of Innovative Research in Science, Engineering and Technology

(An ISO 3297: 2007 Certified Organization)

Vol. 7, Issue 1, January 2018

Recovery of Rare Earth Elements Using Polystyrene and Polysilica Composites and Resulting Depositional Morphologies

Sean Dudley*, William Gleason, Maureen Chorney and Kennedy Southwick

Montana Tech of the University of Montana, Butte, USA

Abstract: This paper examines the recovery of rare earth elements deposited on ion exchange resins. The formation of stabilized metallic structures led to composite particle alteration with polymeric structure, electron availability, pH, kinetics, and f-orbitals playing significant roles in the formation of an organometallic framework affecting access to bonding sites. The depositional morphology of metallic rare earth elements (REE) on the ion exchange resins also showed stabilized metallic structures that led to composite particle destruction. Oxidation/reduction conditions can be used as control mechanisms of the deposition morphologies.

Keywords: Resin, Rare earth, F-orbital, Recovery

I. INTRODUCTION

Researchers at Montana Tech of the University of Montana are looking for cost-effective ways to recover and concentrate rare earth elements (REE). Ion exchange/chelating resins have been widely used by the mining and wastewater industries for selective recovery and concentration of metals. Montana Tech is seeking to expand this technique to REE processing by testing several silica and polystyrene composites having multiple functional groups. Initial investigation showed atypical behavior in resins when loaded with REE instead of transitional metals. When metal REE structures formed on the surface of the ion exchange resins, particle destruction followed in specific cases. Work to characterize the root-causes and mechanisms of metallic deposition and breakage continues.

Previous work at Montana Tech has shown REE self-assembling on both ion exchange and chelating resins. The intent of the experimental phase reported here was to broaden both the spectrum of resins being used and the REE being loaded to determine whether this phenomenon was occurring across the spectrum of resins and REE.

II. MATERIALS AND METHODS

Batch testing used pH-adjusted (2, 5, 8, 10) solutions measured into 20 ml scintillation vials with REE chlorides added to produce concentrations of 1,000 ppm REE. Boundary conditions of pH 2 and pH 10 were used to evaluate the effect of extreme pH, with pH 5 and pH 8 being midpoints. REE chlorides were chosen because chlorine would likely remain a bystander in chemical reactions. The pH conditions changed during testing on the basis of the composite's characteristic functional groups.

Batch testing took place for 48 hours to ensure full loading of the resins. The resins were washed with 19 MΩ water and dried in a low-temperature oven at 80°C. Solutions were analyzed using inductively coupled plasma atomic emission spectroscopy (ICP-AES) with a 21-element multiaxial method. The loaded composite materials were analyzed using scanning electron microscopy (SEM), energy dispersive spectroscopy (EDP), x-ray diffraction, mercury porosimetry, pycnometry, high-resolution light microscopy, x-ray photoelectron spectroscopy, and differential scanning calorimetry.

ISSN(Online): 2319-8753
ISSN (Print): 2347-6710

International Journal of Innovative Research in Science, Engineering and Technology

(An ISO 3297: 2007 Certified Organization)

Vol. 7, Issue 1, January 2018

Batch testing showed uncharacteristic results, primarily particle breakage and uncontrolled metal growth. Column testing was then used to evaluate different loading conditions of gadolinium, neodymium, praseodymium, and yttrium. Conditions were chosen based on the results of batch testing where particle breakage and metallic growth were either present or absent, as well as maximum and minimum adsorption. The columns used an upflow configuration, fed at 3 ml/min (two bed volumes per minute). Table 1 shows the column testing methodology.

Table 1. Column process*.

Step	Action	Approx. Time (min)
1	Wet column with DI water	4
2	Purge air from bed material by pulling vacuum	1
3	Begin pumping REE solution	3
4	Begin taking samples every 30 seconds	10
5	Strip with 4 BV DI water	2
6	Strip with 6 BV 9 N H_2SO_4	3
7	Strip with 4 BV DI water	2
8	Strip with 4 BV 0.5 M NaOH	2
9	Strip with 10 BV DI water	5

* BV = bed volumes; DI = deionized water

Previous research has shown that pH and contact time are the primary means of controlling the adsorption process. Key results of the studies, which in some cases are contradictory, are:

1. Chromium(VI) onto silica – Adsorption qualities are highly dependent on pH conditions [1].
2. Most adsorption occurs within 20 minutes [2].
3. Praseodymium onto pyridine/phosphate – Adsorption rate is governed by interdiffusional kinetics – rates at which elements can travel and find adsorption sites [3].
4. Cerium(III) onto D151 – Higher pH conditions are optimal for, suggesting that adsorption is ion- and ligand-specific [4].
5. Ytterbium(III) onto weak acid gel – Low and high pH conditions inhibit recovery, while optimum recovery was seen at pH 5.5 [5].
6. The adsorption process is dependent on acid (HNO_3) concentration and temperature, indicating that an increase in temperature was not beneficial to adsorption.

Primary analysis for this phase of work consisted of inductively coupled mass spectroscopy and scanning electron microscopy with energy dispersive x-ray spectroscopy. Additional data generated include that from pycnometry and mercury porosimetry.

III. RESULTS

ICP Analysis of Batch Testing

The initial purpose of the project was to evaluate REE for selective removal from solution. Several REE and ion exchange or chelating resins were evaluated. As expected, there was little variation in loading for many of the REE, no matter the resin used. Some elements/resin combinations did show variation, indicating the adsorption characteristics could provide an opportunity for selective recovery. Silica/amine-based resins, for instance, when tested using a light REE (lanthanum) and a heavy REE (holmium) showed such variability. These recovery profiles, shown in Fig. 1, exhibit variable loading (in mg REE/g resin) over the pH range, with maximized recovery conditions occurring at pH 2, 115 mg/g for lanthanum, and pH 8, 95 mg/g for holmium.

ISSN(Online): 2319-8753
ISSN (Print): 2347-6710

International Journal of Innovative Research in Science, Engineering and Technology

(An ISO 3297: 2007 Certified Organization)

Vol. 7, Issue 1, January 2018

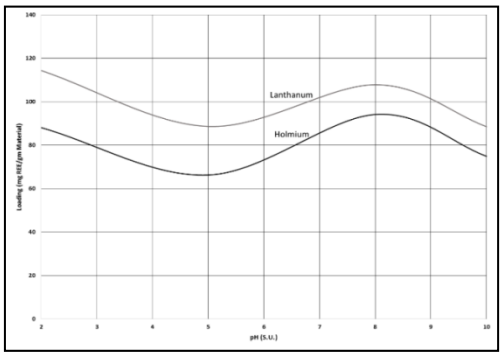

Fig. 1. Loading over altering pH on silica-based resin.

Polystyrene/amine resin loading for several REE are shown in Fig. 2, over a pH range of 2 to 10. Erbium and yttrium are included to show the behavior of nonvariable loading. Yttrium has the greatest recovery at an average of 90 mg/g, but shows no real pH dependence. Neodymium represents a challenge in recovery, averaging 32 mg/g from pH 2 through 8. Cerium and lanthanum show variability that can be manipulated for preferential recovery.

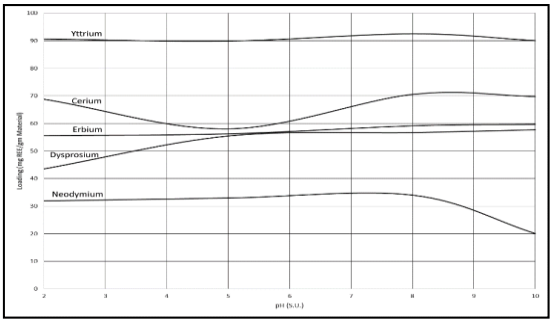

Fig. 2. Loading over altering pH on polystyrene-based resin.

Mercury Porosimetry

Once variation in loading was established, mercury porosimetry was done on the highest loaded silica-based resin for each of the REE to determine porosity changes during loading. An unloaded silica/amine resin was tested, showing a conventional porosity of larger opening pore structure and smaller interior pore structure, as shown in Fig. 3.

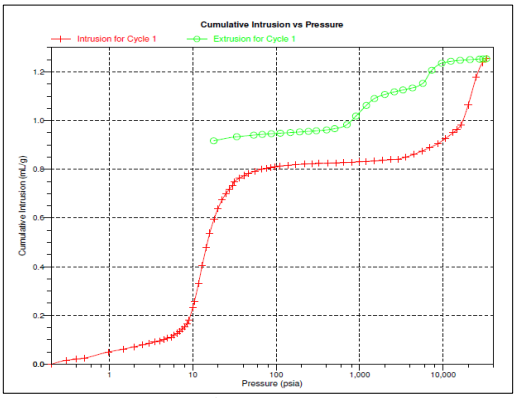

Fig. 3. Cumulative intrusion of mercury in unloaded silica/amine resin.

ISSN(Online): 2319-8753
ISSN (Print): 2347-6710

International Journal of Innovative Research in Science, Engineering and Technology

(An ISO 3297: 2007 Certified Organization)

Vol. 7, Issue 1, January 2018

Once the resin was loaded, the pore structure changed, as shown in Fig. 4. The linear loading at lower pressures showed the larger pores leading to the interior of the resin were equalized while the smaller pores were blocked.

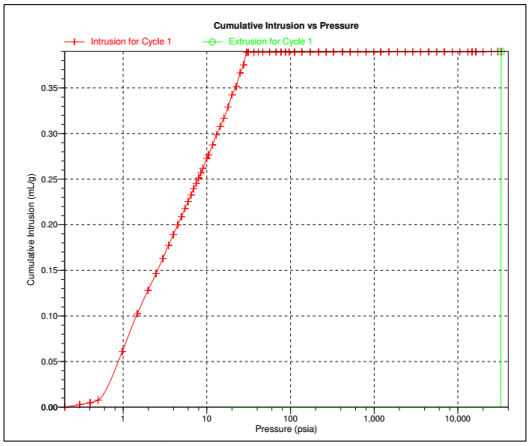

Fig. 4. Cumulative intrusion of mercury in praseodymium-loaded silica/amine resin.

Table 2. Mercury porosimetry data for tested silica resin.

	Si/amine	La (pH 5)	Pr (pH 10)	Dy (pH 5)	Er (pH 5)	Tm (pH 10)
Intrusion volume (ml/g)	1.2534	0.045	0.3897	-0.0119	0.367	1.2181
Pore area (m^2/g)	165.319	28.48	42.7097	0.031	0.104	61.254

Although porosimetry was done on a limited basis, the results exhibited substantial variation in both pore area and mercury intrusion, as shown in Table 2. Some of the REE, such as thulium, affected the resin pore area but not the overall pore volume. Others, such as dysprosium, blocked or eliminated the pore structure. Several intermediary states were also in evidence.

Pycnometry

To further test large-scale resin structure modification, specific gravity (SG) was tested using pycnometry. With REE loading, a resin will increase in density given its increase in mass, although changes should not be substantial, given that REE loading occurs only at functional sites. The SG of silica/amine resin was measured at 1.6, but as in other tests, changes were considerably more than expected. Results of SG, thulium loading, and test pH are shown in Fig. 5.

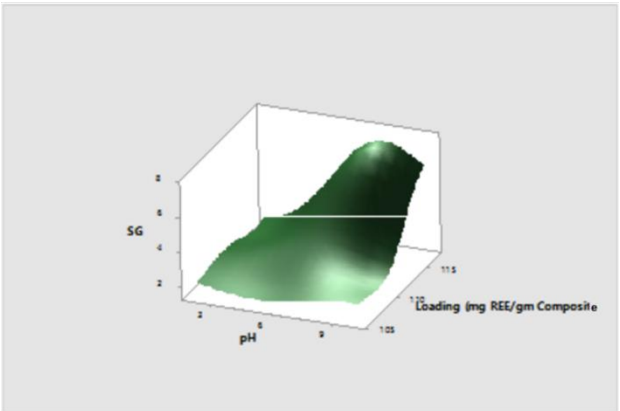

Fig. 5. Specific gravity, pH, and thulium on silica/amine resin.

ISSN(Online): 2319-8753
ISSN (Print): 2347-6710

International Journal of Innovative Research in Science, Engineering and Technology

(An ISO 3297: 2007 Certified Organization)

Vol. 7, Issue 1, January 2018

Resin loading was calculated based on ICP-AES analysis and differed between resins and resin/REE combinations, with light and heavy elements exhibiting differences not only in loading but also behavior. Thulium loading showed a unimodal distribution, much as would be expected, while the light REE cerium loading shown in Fig. 6 exhibited bimodal behavior. Variation between elements were once again in evidence, but results clearly show other variables are involved.

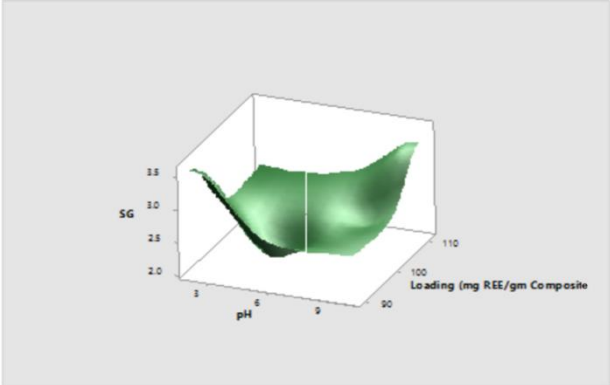

Fig. 6. Specific gravity, pH, and loading of cerium on silica/amine resin.

Differential Scanning Calorimetry Analysis

Calorimetry was used to determine whether the variation seen was reflected in the thermodynamic aspects of resin loading with REE. Variations in calorimetry results were evident. Fig. 7 shows an unloaded silica/amine resin and two resins loaded with dysprosium at two different solution pH. Peak position, line slope, and heat flows were altered when REE loading occurred, indicative of thermodynamic alterations within the general system.

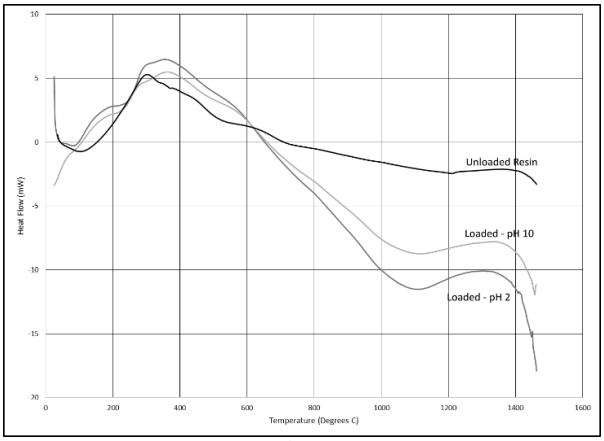

Fig. 7. DSC analysis of dysprosium-loaded resin.

SEM Analysis

Once the presence of substantial alterations in both silica- and polystyrene-based resins were documented, SEM was done to evaluate the physical state of the resins. Initial examination was done using a Phenom SEM (PhenomWorld) capable only of taking backscattered electron images. Loaded composites were compared with their unloaded states to confirm where loading was occurring and if surface modifications were present.

Fig. 8 shows a milled silica/amine resin loaded with cerium. The bottom right of the image shows sheet loading of cerium, particle breakage with staged failure, and secondary REE loading, primarily point source rather than sheet.

ISSN(Online): 2319-8753
ISSN (Print): 2347-6710

International Journal of Innovative Research in Science, Engineering and Technology

(An ISO 3297: 2007 Certified Organization)

Vol. 7, Issue 1, January 2018

Major structural modification is indicated by the particle crack as well as particle agglomeration on the cracked surface. Agglomerations appear to be both caused by and induced by stress cracking, as evidenced by the agglomerations and the bridging seen in the lower left-hand corner of the image.

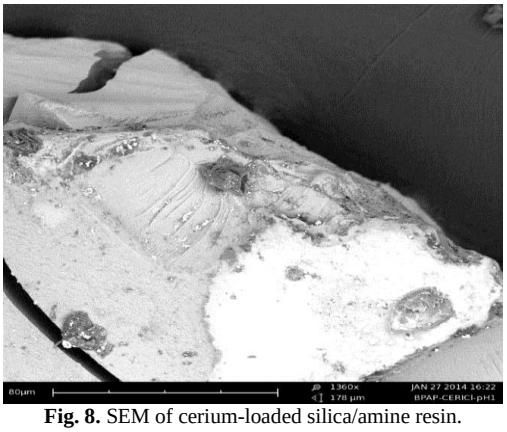

Fig. 8. SEM of cerium-loaded silica/amine resin.

Polystyrene/amine resins were also analyzed. Fig. 9 shows one such resin loaded with dysprosium at pH 2. The polystyrene-based resins are also being compromised as REE load. Note the agglomerated loading on the top particle surface, the interior loading within the break, and the multiple, consistent breaks of the failure itself.

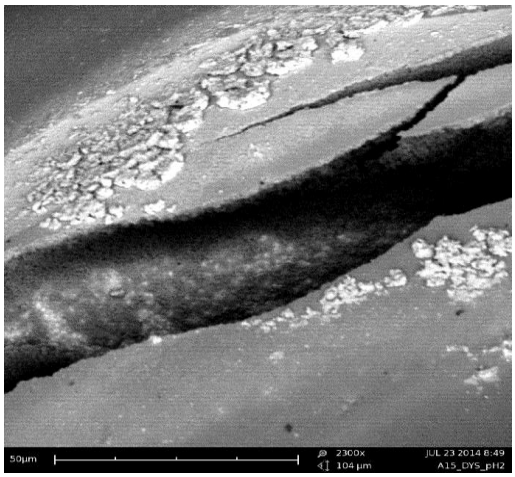

Fig. 9. Polystyrene/amine resin showing breakage and interior loading.

Several depositional morphologies were seen. Depositional morphologies were manipulated using resin, REE, and solution pH. A3 (polystyrene with divinylbenzene functional groups) composite loaded with lanthanum at pH 2 (Fig.10), showed a common morphology of circular surface formations, possibly driven by particle-to-particle contact, with metal infilling occurring once the particles separated in solution.

ISSN(Online): 2319-8753
ISSN (Print): 2347-6710

International Journal of Innovative Research in Science, Engineering and Technology

(An ISO 3297: 2007 Certified Organization)

Vol. 7, Issue 1, January 2018

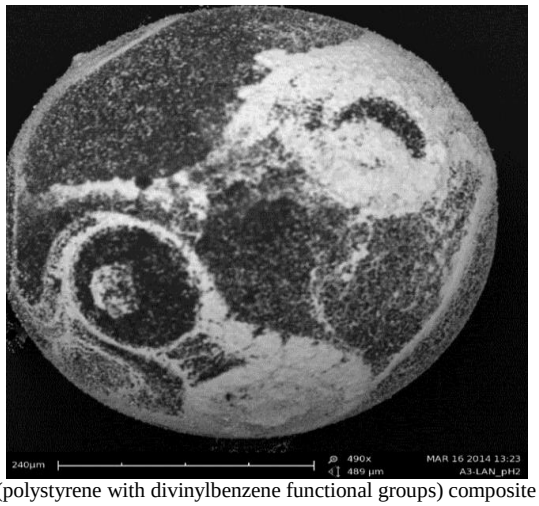

Fig. 10. A3 (polystyrene with divinylbenzene functional groups) composite loaded with lanthanum at pH 2.

Deposition also occurred in rectangular forms, such as occurred in milled A10 (silica with diethylenetriamino functional groups) composite loaded with lanthanum at pH 2 (Fig. 11). Both normal and topographic views of the rectangular stacking morphology are presented. Note the porous growth seen in the upper right hand corner, evidence that more than one morphological structure can occur on the same particle.

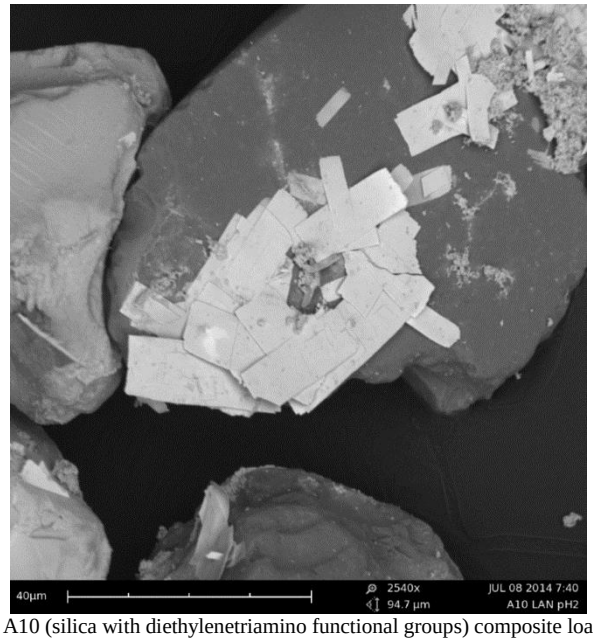

Fig. 11. A10 (silica with diethylenetriamino functional groups) composite loaded with lanthanum at pH 2.

The topographical view shown in Fig. 12 confirms that both the rectangular and the porous formations are growing outward from the structure. Note also that the porous structure appears on several of the rectangular structures, evidence that surface and solution conditions can favour one type of growth over another.

ISSN(Online): 2319-8753
ISSN (Print): 2347-6710

International Journal of Innovative Research in Science, Engineering and Technology

(An ISO 3297: 2007 Certified Organization)

Vol. 7, Issue 1, January 2018

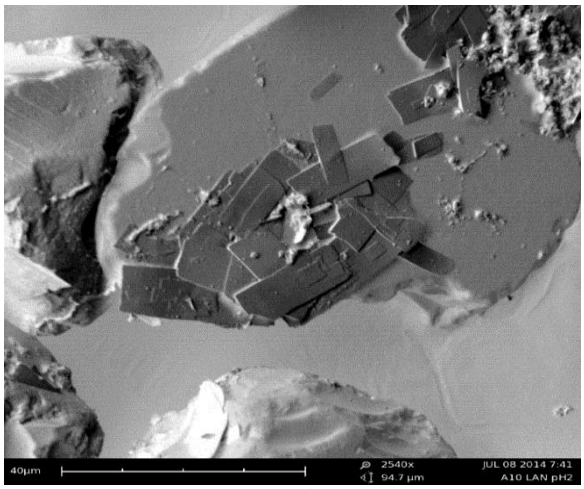

Fig. 12. A10 (silica with diethylenetriamino functional groups) composite loaded with lanthanum at pH 2.

Fig. 13 shows formations on the A5 (polystyrene with aminodiacetic functional groups) composite loaded with lanthanum at pH 5. In this case, nucleation sites are present but growth has occurred in the form of outward sheets on the composite surface. This outward growth was found on a number of polystyrene and silica composite materials, with growths as high as 15 µm documented. The adoption of vertical structures was similar to other metallic formations seen with composite materials in adsorption of europium [3].

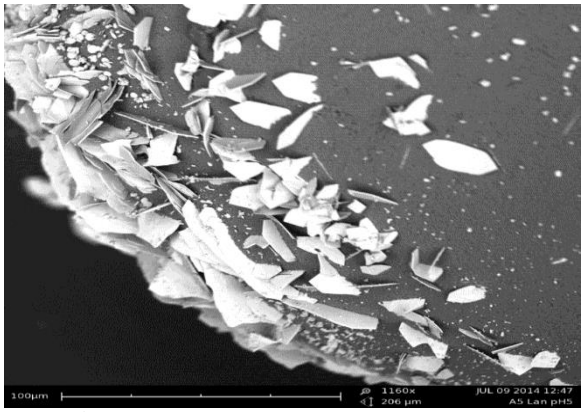

Fig.13. A5 (polystyrene with aminodiacetic functional groups) composite loaded with lanthanum at pH 5 showing surface sheet formation.

The SEM images show a progression of loading and subsequent fracture. The metallic loading resulted in stress localization and breakage along preferred attachment formations or substrate weaknesses. These occurrences were a result of the electronic disruption and metallic nature of the loading. The typical loading mechanism for most adsorption purposes, was point attachment and very little bridging in the form of hydrogen or van der Waals stabilization. These formations showed the transition from point attachment to self-assembling metallic formation.

Again, two important composite modifications can be seen through the use of the SEM analysis. These are consistent with those seen in silica composites. The first is the apparent rupture of the particle, evident from crevices, spalling, or breakage. This is attributed to a multiple stages starting with HOMO-LUMO transitions, the subsequent development of a diffusion pump mechanism stressing pre-existing crazing and final failure of both electronic transfer and substrate.

ISSN(Online): 2319-8753
ISSN (Print): 2347-6710

International Journal of Innovative Research in Science, Engineering and Technology

(An ISO 3297: 2007 Certified Organization)

Vol. 7, Issue 1, January 2018

The other is metal formation on the particle, indicating a second adsorption mechanism. The formation of metallic species indicates that the particle has both organometallic adsorption and metallic adsorption occurring.

IV. DISCUSSION

Our analyses indicated that modifications were occurring to ion exchange resins while being loaded that have not been previously reported in the literature. Results indicated that recovery, separation, and concentration were enhanced by manipulating pH, redox potential, and mechanical conditions with the solution. Additional analyses, including x-ray diffraction, differential scanning calorimetry, SG, porosimetry, and SEM, showed resin modification, including surface and interior pore structure alterations, possible unrestrained metallic formations, and mechanical resin damage. Two important composite modifications – particle rupture and metallic deposition onto the particle – were seen with SEM analysis, whether substrates were polymer or silica based. Numerous SEM images showed a progression of REE loading on the ion exchange/chelating resins, subsequent metallic formation, and, in many cases, particle fracture.

Typical loading mechanisms, for most adsorption purposes, are point attachments at specific engineered sites. Little if any subsequent interaction between loaded sites was reported. The initial atomic REE attachment to the functional site on the ion exchange/chelating resin transitioned from point loading to self-assembling metallic formation, in some cases unrestrained. These formations indicated a second adsorption mechanism. The formations were metallic in nature, indicating that both organometallic adsorption and metallic adsorption were occurring.

Metallic adsorption has not been previously reported. The formation of a metallic structure is of interest because it did not depend on a HOMO-LUMO mechanism; rather, it self-stabilized through a bulk electron transfer, as any other metal is capable of. It is proposed that as the HOMO-LUMO diffusion pump became less predominant, or slowed due to stress and constriction, a secondary mechanism to delocalize charge was activated. This mechanism leads to the formation of metallic structures. That said, the organometallic and metallic regimes still interact with each other and ultimately lead to catastrophic failure. As stated before, further study would need to analyze loading sequences through in-situ atomic force microscopy.

The composites clearly loaded, as determined by ICP analysis, but loading transitioned from a primary functional site attachment to a metallic network formation and final failure. Other analyses, including XRD, DSC, SG, porosimetry, and SEM, indicated that modifications to the ion exchange resins occurred while being loaded. These changes include surface and interior pore structure alterations, possible unrestrained metallic formations, and mechanical resin damage.
SEM image analysis showed that interior loading was occurring, and in some cases overloading the pore structures to the point of rupture. SEM showed that surface deposition was resulting in sheet growth, which may be a contributing factor to surface tension and contraction. Surface cracking, combined with interior pore contraction and rupture, was leading to particle breakage. Porosimetry and SG data support interior loading observations. DSC and XRD support both interior loading and surface loading considerations.

Once sufficient metal has deposited on the surface, a secondary metallic mechanism of delocalized charge is activated, resulting in the unrestrained growth of the metals on the surface. The codependence of these regimes is centered on the ability to transfer an electric charge. The polymer structure initially acts as both a source of electrons and a dispersion network routing electrons to areas at the surface in need of stabilization. The random nature of the underlying polymer network does not allow for consistent stabilization, resulting in localized stress states and charges.
Oxidation-reduction is occurring due to reduced metallic formation, but there are no apparent oxidized species in the solution or polymer. A five-step process is proposed to explain the presence of metallic species:

1. The HOMO-LUMO interaction in polymers, without outside interaction, acts as an initial organic semiconductor process.
2. The reaction energy associated with the REE–organic bond provides a driving force, with additional electronic potential available from the nonreacted end-mers on the polymer chains.

ISSN(Online): 2319-8753
ISSN (Print): 2347-6710

International Journal of Innovative Research in Science, Engineering and Technology

(An ISO 3297: 2007 Certified Organization)

Vol. 7, Issue 1, January 2018

3. The electronic potential effects the available electrons in the REE orbitals once sufficient metal atoms are on the polymer surface as coordinated species.
4. Reduction occurs directly on the surface rather than in the near-surface solution, as the electrons are pumped in manner similar to fuel cell electron transfer.
5. Deposition rates increase as the process continues because more and more bonding sites become available.

The dynamic nature of metallic interaction with organic frameworks is evidenced in gold nanoparticles experimentation were controlled through strict procedures using capping agents and reducing agents, and block copolymers have displayed a metal-reducing function and self-stabilizing ability [6]. Although the reduction of gold is in a different realm compared with REE, the ability of a metal to self-reduce and self-regulate chemical stability is a basis upon which arguments can be built. The metal–organic framework interface is dependent on that underlying structure. [7] In addition, it has been demonstrated that the variable coordination numbers exhibited by REE metals give them a higher affinity for hard donor atoms [8].

This type of behavior is a necessary step to building a linked metal structure on the surface of the polymer. The f-orbital's ability to accommodate multiple conformations is a primary driver for creating the electronic network that stabilizes REE on polymeric structures.

In lanthanide and actinide separation, observed Nash et al., "separations are based on the contribution of ligand donor atoms softer (i.e., more polarizable) than oxygen." [9]. This statement sets the baseline that fundamental adsorption starts with polarized ligands. Nash et al. hypothesized that subsequent polarized metallic constituents continue the deposition process.

The effect of pH examined in this paper illustrates that the near-surface REE solution conditions dictate the nature of metal deposition onto the polymer. REE chlorides provide both positive and negative charges to the working solution, but the excess hydronium limits the very large REE ion movement, requiring complex restructuring of the near-surface solution as the metal ions move toward the surface, first to coordinate selectively with the functionalized end of the polymer and then to begin and sustain the metallic deposition. As the solution moves to the hydroxide regime, this behavior changes to a more robust delivery as the polymer surface releases hydrogen, which reacts with hydroxide while the REE ion coordinates at the surface.

Once the hydrogen release is complete and the coordination is ending, the REE ions can move in large numbers to reduce on the surface itself. The first result is a more structured deposition onto the surface, while the second is a bulk deposition near the surface.

V. CONCLUSION

ICP-AES data indicates that separation and concentration of REE using ion exchange resin technology is possible. X-ray diffraction, differential scanning calorimetry, SG, porosimetry, SEM, and EDS have been used to elucidate chemical interactions between REE and the resin structure. Anomalous particle behavior has been seen occurring over a wide range of conditions. These conditions are basic and fundamental to any operation meant to recover REE using ion exchange or chelating resins. We suspect that widespread alteration of the interior pore structure is leading to several elevated stress states. These stresses contort the interior pore walls, leading to localized rupture based on existing substrate flaws that starts a chain of ruptures, and results in particle breakdown.

Attachment and growth occurs first on the atomic scale then transitions to a nanoscale phenomenon, but can extend to the microscale and possibly the macroscale. This extension is limited only by the capability of the internal networks, both ionic and electronic, to transfer electrons and possibly ions within the structure, as well as the external surrounding's ability to supply REE to the surface. With modification, it should be possible to form stable anode-like structures.

ISSN(Online): 2319-8753
ISSN (Print): 2347-6710

International Journal of Innovative Research in Science, Engineering and Technology

(An ISO 3297: 2007 Certified Organization)

Vol. 7, Issue 1, January 2018

HOMO-LUMO theory and the f-orbitals in organometallic frameworks are proposed to explain the initiation of electron transfer and on-surface reduction seen in this project. A key component to the problem presented is that the bonding and electron transfer of REE and organic frameworks is centered on the f-orbital. This orbital is little studied and its interaction on the HOMO-LUMO front is little understood. This work does not propose a new framework for electronic sharing or bonding, but rather a possible explanation for our observations. These "unique coordination characteristics" and "exceptional optical and magnetic properties arising from 4-f electrons," [10] and the dynamic nature of the organometallic framework, pose a new frontier for materials science. Continued development of these exceptional qualities can bring new materials to market.

Acknowledgement

Research was sponsored by the Army Research Laboratory and was accomplished under Cooperative Agreement Number W911NF-15-2-0020. The views and conclusions contained in this document are those of the authors and should not be interpreted as representing the official policies, either expressed or implied, of the Army Research Laboratory or the U.S. Government. The U.S. Government is authorized to reproduce and distribute reprints for Government purposes notwithstanding any copyright notation herein.

REFERENCES

[1] J. Qui, Z. Wang, H. Li, L. Xu, J. Peng, M. Zhai, C. Yang, J. Li, G. Wei, "Adsorption of Cr(VI) using silica based adsorbent prepared by radiation-induced grafting," Journal of Hazardous Materials vol. 166 no.1, pp.270-276, 2009.
[2] Z. Wang, C. Ye, X. Wang, J. Li, "Adsorption and desorption characteristics of imidazole-modified silica for chromium (VI)," Applied Surface Science vol. 287, pp. 232-241, 2013.
[3] C. Xiong, J. Zhu, S. Chen, Q. Chen, "Adsorption and desorption of praseodymium (III) from aqueous solution using D72 resin," Separation Science and Engineering, vol. 20 no.5, pp.823-830, 2012.
[4] C. Yao, "Adsorption and desorption properties of D151 resin for Ce (III)," Journal of Rare Earths, vol. 28 (Suppl. 1), pp.183-188, 2010.
[5] Z. Zheng, C. Xiong, "Adsorption behavior of ytterbium(III) on gel-type weak acid resin," Journal of Rare Earths vol. 29 no.5, pp.407-412, 2011.
[6] T. Sakai, Y. Horiuchi, P. Alexandridis, T. Okada, S. Mishima, "Block co-polymer mediated synthesis of gold nanoparticles in aqueous solutions: Segment effect on gold ion reduction, stabilization, and particle morphology," Journal of Colloid and Interface Science vol. 394, pp.124-131, 2013.
[7] RC. Scaravelli, RL. Dazzi, FC. Giacomelli, G. Machado, C. Giacomelli, V. Schmidt, "Direct Synthesis of coated gold nanoparticles mediated by polymers with amino groups," Journal of Colloid and Interface Science, vol. 397, pp.114-21, 2013.
[8] B. Li, H.M. Wen, Y. Cui, G. Qian, B. Chen, "Multifunctional lanthanide coordination polymers," Progress in Polymer Science 48:40-84, 2015.
[9] K. Nash, C. Madic, J.N. Mathur, J. Lacquement, "Actinide separation science and technology", The Chemistry of the Actinide and Transactinide Elements vol. 4, pp. 2622-2798, 2016.
[10] G. Zhuang, W. Chen, J. Zheng, H. Yu, J. Wang, "N-(sulfoethyl) iminodiacetic acid-based lanthanide coordination polymers: Synthesis, magnetism and quantum Monte Carlo Studies", Journal of Solid State Chemistry vol. 192, pp.284-288, 2012.